Modified-Energy Management of Multiple Microgrid

Yi Zhao[1,2(✉)] and Jilai Yu[1]

[1] School of Electrical Engineering and Automation,
Harbin Institute of Technology, Harbin 150001, Heilongjiang, China
reef6l4@l63.com
[2] School of Electric Power, Shenyang Institute of Engineering, Shenyang, China

Abstract. This paper presented an energy management model for managing an active distribution network (ADN) consisting of multiple microgrids. The distribution system operator (DSO) of the ADN needs to coordinate the microgrids to achieve optimal energy management. This paper formulated the energy management of ADN with multiple microgrids as a mixed integer second-order cone programming (MISOCP), which considered network reconfiguration, on-load tap changer (OLTC) and static Var compensators (SVC). A case study on a modified IEEE 33-bus distribution network demonstrates the effectiveness of the proposed method.

Keywords: Active power distribution network · Energy management · Multiple microgrids

1 Introduction

Driven by the rapid development and integration of distributed energy resources (DERs), the distribution network is evolving towards active distribution network (ADN). Microgrid technology has been widely recognized as an effective means of integrating distributed generation, energy storage such that it is friendly and controllable to the distribution network [1]. DERs clustered in a microgrid include non-controllable renewable generators, controllable conventional generators, energy storage devices, etc. Each microgrid has a central controller which has two-way communication with the DERs and controls their operation as well as the power exchange between microgrid and externa utility grid. Networked microgrids can supply their local power demands not only by their on-site resources but also by the external supply from the remaining part of the ADN [2]. These networked microgrids can also provide ancillary services to the ADN [3, 4].

In the ADN, the MGCCs and DSO are different parities seeking for their own individual interests. The energy management in ADNs involves multi-party decision making, forming a complex optimization problem. Each decision maker has separate observability and controllability in the whole distribution network [5]. Traditionally, centralized optimization models are used for the energy management of DSO to coordinate the operations of microgrids and the ADN. In this context, the DSO needs to have full observability and controllability on all of the DERs in microgrids. However,

H. Gao et al. (Eds.): TridentCom 2019, LNICST 309, pp. 95–106, 2020.
https://doi.org/10.1007/978-3-030-43215-7_7

the centralized fashion is facing new challenges [6, 7]. The MGCCs and DSO are independent parties with different interests so that they may not be willing to share private or sensitive information with each other [8, 9]. In addition, with integrating all the DERs in microgrids into the centralized model of DSO, the complexity and problem size will increase dramatically, making the model much more complicated and difficult to solve. Therefore, we need to consider the coordination between the DSO and MGCCs in the energy management for ADNs to overcome these challenges and meanwhile retain the same quality of optimal solutions [10, 11].

The most prominent appearance of high permeability of multiple microgrids is that it brings greater variability and uncertainty to the site selection, constant capacity and real-time output of microgrid, increasing the risk of congestion of active power flow and uneven distribution of reactive power flow in distribution network. The high degree of autonomy of the cast and cast behavior in the normal and accident conditions of the multiple microgrids aggravates the uncertainty and risk. Due to the unidirectivity of protection configuration, the distribution network should have the characteristics of closed-loop design and open-loop operation. This paper proposed an optimal energy management framework for AND based on MISOCP, consisting of multiple networked microgrids. It aimed at achieving energy management in an ADN while comprehensively considering the security constraint, advanced control strategies, such as OLTC, SVC, network reconfiguration, etc.

2 Energy Management in Active Distribution Network with Multiple Microgrids

A MISOCP-based security-constrained economic dispatch model is proposed for the energy management of active distribution networks with multiple microgrids. Here the single-period operation [12] of an ADN is considered. The energy management of the DSO and MGCCs is shown in Fig. 1.

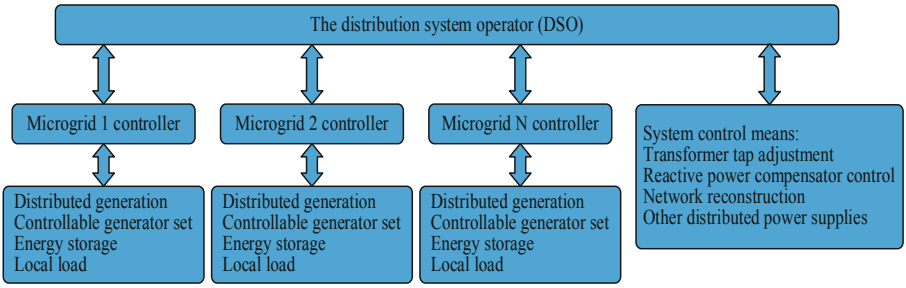

Fig. 1. Energy management of multiple microgrids in ADNs.

2.1 Power Flow Model of ADN with Network Reconfiguration

The distribution network usually has a radial topology, for which DistFlow model was proposed in [12] to simplify the conventional full AC power flow model. According to the DistFlow model, the line flow and node injections related to node m can be written as:

$$P_{I,m} = p_{mn_1} + p_{mn_2} - (p_{km} - r_{km} l_{km}) \tag{1}$$

$$Q_{I,m} = q_{mn_1} + q_{mn_2} - (q_{km} - x_{km} l_{km}) \tag{2}$$

$$v_k - v_m = 2(r_{km} p_{km} + x_{km} q_{km}) - \left(r_{km}^2 + x_{km}^2\right) l_{km} \tag{3}$$

$$p_{km}^2 + q_{km}^2 = v_k l_{km} \tag{4}$$

In the above model, Eqs. (1) and (2) are the nodal balance equations for active and reactive power at node m, respectively. Equation (3) describes the voltage drop equation between the two end nodes of the distribution line. Equation (4) describes the relationship among voltage, current, active power and reactive power.

To convexify Eq. (4), SOC relaxation is applied and Eq. (4) is converted into the following SOC form.

$$p_{km}^2 + q_{km}^2 \le v_k l_{km} \tag{5}$$

Equation (5) is a rotated quadratic cone. The exactness of this SOC relaxation has been proved.

2.2 On-load Tap Changer (OLTC)

On-load tap changer (OLTC) is an important means in distribution network to regulate the voltage. The DSO can adjust the tap position of the transformers to control the voltage over the network. In this paper, we introduce a dummy bus named as k′ and add into the bus set Ω. Then the transformer can be modeled as a distribution line kk′ and added into the distribution line set Ψ_{NS} and a series connected tap changer k′m included in the transformer set Ψ_T. At each line representing the transformer, we have the following equation regarding the two nodal voltages.

$$v_{k'} = \eta_{km}^2 v_m, \ \forall (k', m) \in \mathbf{\Psi}_T \tag{6}$$

where the tap changing ratio is represented by:

$$\eta_{km} = \underline{\eta}_{km} + \kappa_{km} T_{km}, \ \ \forall (k', m) \in \mathbf{\Psi}_T \tag{7}$$

and the tap position can be modeled as an integer:

$$0 \le \kappa_{km} \le \frac{\bar{\eta}_{km} - \underline{\eta}_{km}}{T_{km}}, \quad \forall (k', m) \in \mathbf{\Psi}_{\mathrm{T}} \tag{8}$$

Using binary expansion, we can further represent the tap position by the following equation.

$$\kappa_{km} = \sum\nolimits_{h=0}^{H_{km}} 2^h \alpha_{km,h}, \quad \forall (k', m) \in \mathbf{\Psi}_{\mathrm{T}} \tag{9}$$

The value H_{km} can be determined by Eq. (10).

$$\sum\nolimits_{h=0}^{H_{km}-1} 2^h < \frac{\bar{\eta}_{km} - \underline{\eta}_{km}}{T_{km}} \le \sum\nolimits_{h=0}^{H_{km}} 2^h, \quad \forall (k', m) \in \mathbf{\Psi}_{\mathrm{T}} \tag{10}$$

It can be observed that, by substituting (6) and (7), Eq. (9) will contain a number of products of continuous and binary variables, which is highly non-linear and will increase the computational complexity significantly. To address this issue, we introduce auxiliary variables $\alpha_{km,h}$, $\beta_{km,h}$, and $\gamma_{km,h}$ to replace the nonlinear terms, and then the following set of equations [12] are written in (11a–11f), which is equivalent to Eq. (6).

$$v_{k'} = \underline{\eta}_{km} \delta_{km} + T_{km} \sum\nolimits_{h=0}^{H_{km}} 2^h \gamma_{km,h}, \quad \forall (k', m) \in \mathbf{\Psi}_{\mathrm{T}} \tag{11a}$$

$$\delta_{km} = \underline{\eta}_{km} v_m + T_{km} \sum\nolimits_{h=0}^{H_{km}} 2^h \beta_{km,h}, \quad \forall (k', m) \in \mathbf{\Psi}_{\mathrm{T}} \tag{11b}$$

$$0 \le v_{m,t} - \beta_{km,h} \le \bar{v}_m (1 - \alpha_{km,h}), \quad \forall h, \forall (k', m) \in \mathbf{\Psi}_{\mathrm{T}} \tag{11c}$$

$$0 \le \beta_{km,h} \le \bar{v}_m \alpha_{km,h}, \quad \forall h, \forall (k', m) \in \mathbf{\Psi}_{\mathrm{T}} \tag{11d}$$

$$0 \le \delta_{km} - \gamma_{km,h} \le \bar{v}_m \bar{\eta}_{km} (1 - \alpha_{km,h}), \quad \forall h, \forall (k', m) \in \mathbf{\Psi}_{\mathrm{T}} \tag{11e}$$

$$0 \le \gamma_{km,h} \le \bar{v}_m \bar{\eta}_{km} \alpha_{km,h}, \quad \forall h, \forall (k', m) \in \mathbf{\Psi}_{\mathrm{T}} \tag{11f}$$

where δ_{km} is an auxiliary variable representing voltage magnitude.

3 Energy Management Model of Active Distribution Network with Multiple Microgrids

The network energy management of active power distribution with multiple microgrids can be divided into two layers. The upper layer is the energy management of the active distribution network. The lower layer considers the power exchange with the distribution network for each sub-microgrid and performs optimal scheduling of local power generation resources and loads.

3.1 Energy Management of DSO

The active and reactive power exchange between the networked microgrids and the ADN need to meet the constraints as follows.

$$P_{I,m} = P_{X,m}, \quad Q_{I,m} = Q_{X,m}, \quad \forall m \in \mathbf{\Omega}_{\mathrm{M}} \tag{12}$$

$$\underline{P}_{X,m} \le P_{X,m} \le \bar{P}_{X,m}, \quad \underline{Q}_{X,m} \le Q_{X,m} \le \bar{Q}_{X,m}, \quad \forall m \in \mathbf{\Omega}_{\mathrm{M}} \tag{13}$$

Equation (12) defines the active and reactive power flows from the microgrids to the ADN. Equation (13) enforces the lower and upper limits of the power exchange.

The load curtailments at non-microgrid nodes are subject to the constraints below.

$$0 \le P_{LS,m} \le P_{D,m}, \quad \forall m \in \mathbf{\Omega} \backslash \mathbf{\Omega}_{\mathrm{M}} \tag{14}$$

$$P_{LS,m} Q_{D,m} = Q_{LS,m} P_{D,m}, \quad \forall m \in \mathbf{\Omega} \backslash \mathbf{\Omega}_{\mathrm{M}} \tag{15}$$

Equation (14) represent the limit of active power demand curtailment at non-microgrid buses. Equation (15) is representing that the curtailment of load demand will not affect the power factor at this node.

According to the above model, the net power injections at each non-microgrid bus in the ADN can be formulated as follows.

$$P_{I,m} = P_{B,m} - P_{D,m} + P_{LS,m}, \quad \forall m \in \mathbf{\Omega}_{\mathrm{B}} \tag{16}$$

$$P_{I,m} = -P_{D,m}, \quad \forall m \in \mathbf{\Omega} \backslash \{\mathbf{\Omega}_{\mathrm{B}} \cup \mathbf{\Omega}_{\mathrm{M}}\} \tag{17}$$

$$Q_{I,m} = Q_{B,m} - Q_{D,m} + Q_{LS,m}, \quad \forall m \in \mathbf{\Omega}_{\mathrm{B}} \tag{18}$$

$$Q_{I,m} = Q_{S,m} - Q_{D,m} + Q_{LS,m}, \quad \forall m \in \mathbf{\Omega}_{\mathrm{S}} \tag{19}$$

$$\underline{Q}_{S,m} \le Q_{S,m} \le \bar{Q}_{S,m}, \quad \forall m \in \mathbf{\Omega}_{\mathrm{S}} \tag{20}$$

$$Q_{I,m} = -Q_{D,m} + Q_{LS,m}, \quad \forall m \in \mathbf{\Omega} \backslash \{\mathbf{\Omega}_{\mathrm{M}} \cup \mathbf{\Omega}_{\mathrm{S}} \cup \mathbf{\Omega}_{\mathrm{B}}\} \tag{21}$$

Equations (16) and (18) represent active and reactive power injections at the buses on the boundary; Eq. (17) shows the injected active power at the buses that are neither the external transmission network nor a microgrid and has no distributed energy resources; Eq. (19) indicates the injected reactive power at the buses with SVCs. Equation (27) represents the models of SVS with continuous adjustment of reactive power output; (21) represents reactive power injection at the buses without SVCs.

The operation costs of networked microgrids C_{mg}, including power exchange and production, are calculated by the MGCCs. The DSO will consider the following costs of buying power from transmission power grid C_{imp} and load shedding C_{shed}.

$$C_{imp} = \sum_{m \in \mathbf{\Omega}_{\mathrm{B}}} \rho_{E,m} P_{B,m} \tag{22}$$

$$C_{shed} = \sum_{m \in \mathbf{\Omega} \backslash \mathbf{\Omega}_{\mathrm{M}}} \rho_{LS} P_{LS,m} \tag{23}$$

It is noted that load curtailment is the last action that the DSO makes to maintain supply-demand balance, so ρ_{LS} is set to be a value that is much larger than $\rho_{E,m}$ $(\forall m \in \mathbf{\Omega}_{\mathrm{B}})$.

The operational security constraints including line flow and voltage limits are shown as follows.

$$p_{km}^2 + q_{km}^2 \leq S_{km}^2, \quad \forall (k,m) \in \mathbf{\Psi} \tag{24}$$

$$\underline{v}_m \leq v_m \leq \bar{v}_m, \quad \forall m \in \mathbf{\Omega} \backslash \mathbf{\Omega}_{\mathrm{B}} \tag{25}$$

$$v_m = \tilde{v}_m, \quad \forall m \in \mathbf{\Omega}_{\mathrm{B}} \tag{26}$$

Equation (24) indicates the line flow capacity limits. Equation (25) is the voltage limit on each node and Eq. (26) enforces that the voltage magnitude of substation nodes are equal to preset values.

To minimize the voltage deviation from the nominal voltage, a penalty term is included to represent the cost of accumulated deviations.

$$C_{vol} = \rho_V \sum_{m \in \mathbf{\Omega}} \upsilon_m \tag{27}$$

where υ_m is defined as

$$\upsilon_m = |v_m - \tilde{v}_m|, \quad \forall m \in \mathbf{\Omega} \tag{28}$$

In addition, Eq. (28) can be converted to the following two constraints by eliminating the absolute value operator.

$$\upsilon_m \geq v_m - \tilde{v}_m, \quad \forall m \in \mathbf{\Omega} \tag{29}$$

$$\upsilon_m \geq \tilde{v}_m - v_m, \quad \forall m \in \mathbf{\Omega} \tag{30}$$

3.2 Energy Management of Individual Microgrids

The microgrids operate a number of dispatchable generation resources to serve their local load demands and exchange power with ADN. The central controller of the microgrid, MGCC, will conduct energy management based on the operational characteristics of its disputable distributed energy resources. The renewable-based and dispatchable generators are modelled as follows.

$$\underline{P}_{G,g} \le P_{G,g} \le \bar{P}_{G,g}, \quad \forall g \in \mathbf{\Pi}_{\mathrm{C},m} \tag{31}$$

$$P_{G,g} = \tilde{P}_{G,g}, \quad \forall g \in \mathbf{\Pi}_{\mathrm{R},m} \tag{32}$$

Equation (31) enforces upper and lower generation limits on dispatchable units. To maximize the utilization of renewable generation, Eq. (32) sets the active power output of the renewable generators to be the forecasted values.

In the microgrid, energy storage system is used to smooth the variations of active power consumption and renewable power generation by discharging and charging management, which can be modelled as follows.

$$-\bar{P}_{E,e} \le P_{Ch,e} - P_{Dch,e} \le \bar{P}_{E,e}, \quad \forall e \in \mathbf{\Lambda}_m \tag{33}$$

$$\underline{E}_e \le \tilde{E}_e + \xi_e P_{Ch,e} - \frac{1}{\zeta_e} P_{Dch,e} \le \bar{E}_e, \quad \forall e \in \mathbf{\Lambda}_m \tag{34}$$

$$P_{Ch,e} \ge 0, P_{Dch,e} \ge 0, \quad \forall e \in \mathbf{\Lambda}_m \tag{35}$$

Equation (33) indicates the maximum charging and discharging power limits. Equation (34) describes that the energy remained in the energy storage should respect the upper and lower limits. Equation (35) enforces the charging and discharging power to be non-negative.

In addition, the controllable units can provide reactive power by smart inverters. The reactive power output constraint is expressed as.

$$\underline{Q}_{G,m} \le Q_{G,m} \le \bar{Q}_{G,m} \tag{36}$$

where $Q_{G,m}$ is the reactive power output of the generator m, $\underline{Q}_{G,m}$ and $\underline{Q}_{G,m}$ is the lower and upper limits.

Part of the load demand in the microgrid is interruptible or adjustable, so we consider load curtailment in the energy management of MGCC, expressed as the following equtions.

$$0 \le P_{LS,m} \le P_{D,m} \tag{37}$$

$$P_{LS,m} Q_{D,m} = Q_{LS,m} P_{D,m} \tag{38}$$

Equation (38) indicates that the curtailment of active and reactive power load demands will not affect the power factor.

The active and reactive power balances in the microgrid need to be maintain by the MGCC, shown in Eq. (39) and (40) respectively.

$$\sum_{g \in \mathbf{\Pi}_m} P_{G,g} + \sum_{e \in \mathbf{\Lambda}_m} \left(P_{Dch,e} - P_{Ch,e} \right) = P_{X,m} + P_{D,m} - P_{LS,m} \tag{39}$$

$$\sum_{g\in\mathbf{\Pi}_m} Q_{G,g} = Q_{X,m} + Q_{D,m} - Q_{LS,m} \tag{40}$$

The operation costs of a microgrid includes the generation cost of controllable generator, load curtailment cost and deprecation cost of energy storage while assuming that the generation cost of renewable generator is close to zero. The generation cost curve of a controllable generator is modelled in a quadratic function.

$$C_{gen,m} = \sum_{g\in\mathbf{\Pi}_{C,m}} \left(a_g P_{G,g}^2 + b_g P_{G,g} + c_g\right) \tag{41}$$

The load curtailment cost is expressed as

$$C_{shed,m} = \rho_{LS} P_{LS,m} \tag{42}$$

The charging and discharging of energy storage will cause the depreciation of energy storage and impact its lifetime. The depreciation cost of energy storage devices are modelled as

$$C_{deg,m} = \sum_{e\in\mathbf{\Lambda}_m} a_e \left[\left(P_{Ch,e}\right)^2 + \left(P_{Dch,e}\right)^2\right] \tag{43}$$

The above capacity degradation coset model is a quadratic function that has been verified in [7] using experimental data.

3.3 Energy Management of ADN with Multiple Microgrids

In summary, the optimization model of the energy management of the DSO and multiple MGCCs is formulated as an MISOCP problem as follows. The DSO will solve the optimization model to make optimal decisions in the ADN and the MGCCs of the microgrids will follow the DSO's commands in order to collaborate with each other to achieve the overall optimal operation of the ADN:

$$\min\ C_{imp} + C_{shed} + C_{vol} + C_{mg} \tag{44}$$

$$\text{s.t. } C_{mg} = \sum_{m\in\mathbf{\Omega}_M} \left(C_{gen,m} + C_{shed,m} + C_{deg,m}\right) \tag{45}$$

In this model, the objective aims at minimizing the total operation cost of the ADN with considerations of the physical and operational constraints of the ADN and microgrids.

4 Case Studies

In this section, the case study is carried out on a modified IEEE 33-bus distribution system. The proposed model and algorithm are implemented in MATLAB 2016a with the commercial solver MOSEK 8.1 on a personal computer with 2.4 GHz CPU and 12G RAM. In the mixed integer programming, the relative optimality gap is set at 0.01% by default.

4.1 System Description

A modified IEEE 33-node distribution system is used to test the proposed model [12]. The operational data of the dispatchable generators and energy storage devices in the microgrids are listed in Tables 1 and 2. The data of renewable power generation, load demand and reactive power generation in each microgrid are given in Table 3. The base-case network topology is given in Fig. 2 and the three microgrids are located at node 13, 18 and 30, respectively. Two SVCs are at node 12 and 28, repectively [13, 14].

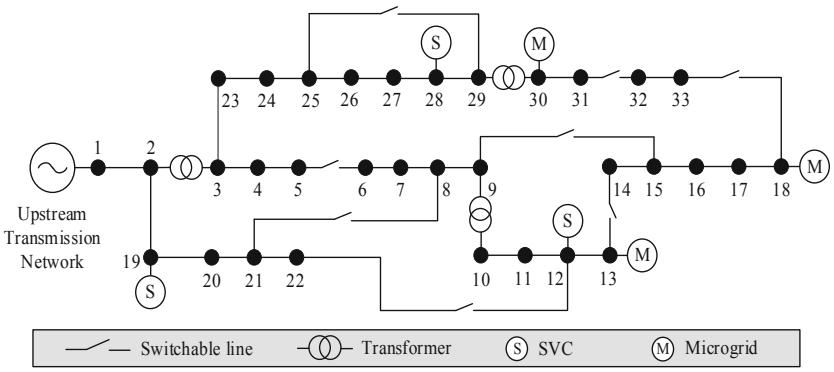

Fig. 2. Test power distribution system in the base case.

Table 1. Controllable generation units in the three microgrids.

Bus	Technical parameters		Cost coefficients		
	Min output (kW)	Max output (kW)	a ($/(MW)2 h)	b ($/MWh)	c ($/h)
13	50	300	0.5	10	5
18	100	500	1.2	15	3
30	100	500	0.8	12	4

Table 2. Energy storage devices in the three microgrids.

Bus	Max power (kW)	Energy level (kWh)		
		Min	Max	Initial
13	50	50	200	100
18	100	100	300	100
30	100	100	300	200

Table 3. Onsite load and resources in the three microgrids.

Bus	Power demand		Renewable resource (kW)
	Real (kW)	Reactive (kVar)	
13	350	200	0.9/0.9
18	400	300	0.9/0.9
30	500	800	0.85/0.85

4.2 Results

The optimal power exchange schedules of the three micgrogrids in ADN under 10 different scenarios with different load levels by the proposed model are shown in Fig. 3, and the total cost is given in Fig. 4.

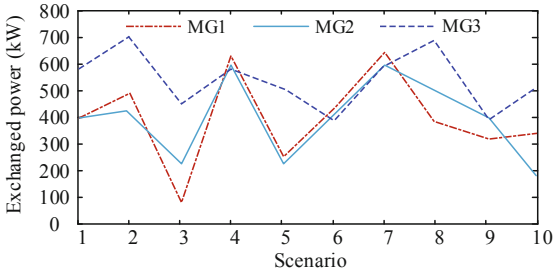

Fig. 3. Optimal power exchange schedules of the three microgrids (MG 1–3) in AND under different scenarios.

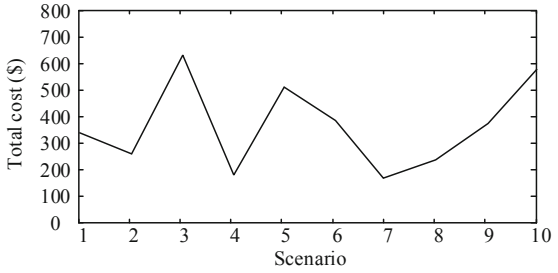

Fig. 4. Total cost of the three microgrids (MG 1–3) in AND under different scenarios.

Then we study the impact of exchange limit of microgrid on the optimal exchange schedules. By changing the exchange limit from 500 kVA to 100 kVA, Fig. 5 shows the variations of the microgrid tie-line flow schedules and Fig. 6 gives the total cost.

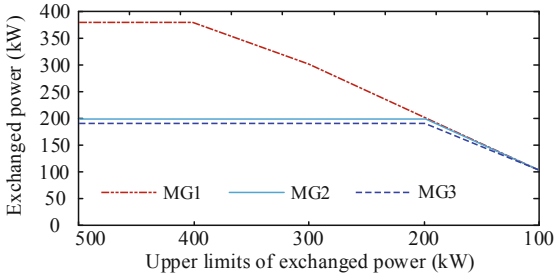

Fig. 5. Optimal power exchange schedules of the three microgrids (MG 1–3) in ADN under different exchange limits of microgrids.

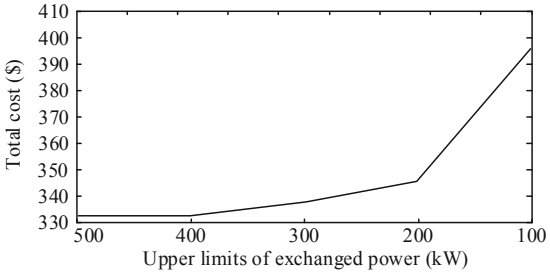

Fig. 6. Total cost of the three microgrids (MG 1–3) in AND under different exchange limits of microgrids.

It can be observed from Fig. 6 that with the decrease of the microgrid exchange limit, the total cost increases. When the limit is decreased to 300 kVA, the microgrid exchange power will be limited by these constraints and capped at the maximum exchange limit.

5 Conclusion

In this paper, the connection switch of the transfer line is used to realize the network reconstruction under the radial structure of the distribution network so as to reduce the line loss and eliminate the line obstruction. The influence of ADN reconstruction and OLTC transformer operation is considered, and the model realizes the highly autonomous cooperative optimal operation domain control between the microgrids and the distribution network. IEEE 33 bus example shows that the strategy can effectively realize the economic operation in the distribution network.

References

1. Feng, C., Li, Z., Shahidehpour, M., Wen, F., Liu, W., Wang, X.: Decentralized short-term voltage control in active power distribution systems. IEEE Trans. Smart Grid **9**, 4566–4576 (2017)
2. Koutsoukis, N.C., Siagkas, Di.O., Georgilakis, P.S., Hatziargyriou, N.D.: Online reconfiguration of active distribution networks for maximum integration of distributed generation. IEEE Trans. Autom. Sci. Eng. **14**(2), 437–448 (2017)
3. Li, Z., Shahidehpour, M., Aminifar, F., Alabdulwahab, A., Al-Turki, Y.: Networked microgrids for enhancing the power system resilience. Proc. IEEE **105**(7), 1289–1310 (2017)
4. Wang, H., Huang, J.: Incentivizing energy trading for interconnected microgrids. IEEE Trans. Smart Grid **9**, 2647–2657 (2016)
5. Ma, W.-J., Wang, J., Gupta, V., Chen, C.: Distributed energy management for networked microgrids using online alternating direction method of multipliers with regret. IEEE Trans. Smart Grid **9**, 847–856 (2016)
6. Liu, T., et al.: Energy management of cooperative microgrids: a distributed optimization approach. Int. J. Electr. Power Energy Syst. **96**, 335–346 (2018)
7. Liu, Y., et al.: Distributed robust energy management of a multi-microgrid system in the real-time energy market. IEEE Trans. Sustain. Energy **10**, 396–406 (2017)
8. Malekpour, A.R., Pahwa, A.: Stochastic networked microgrid energy management with correlated wind generators. IEEE Trans. Power Syst. **32**(5), 3681–3693 (2017)
9. Qi, C., et al.: A decentralized optimal operation of AC/DC hybrid distribution grids. IEEE Trans. Smart Grid **9**, 6095–6105 (2017)
10. Wu, L.: A transformation-based multi-area dynamic economic dispatch approach for preserving information privacy of individual areas. IEEE Trans. Smart Grid **10**, 722–731 (2017)
11. Gregoratti, D., Matamoros, J.: Distributed energy trading: the multiple-microgrid case. IEEE Trans. Ind. Electron. **62**(4), 2551–2559 (2015)
12. Baran, M.E., Wu, F.F.: Network reconfiguration in distribution systems for loss reduction and load balancing. IEEE Trans. Power Deliv. **4**(2), 1401–1407 (1989)
13. Setiasih, Suyatno, T.: The effect of product mix and lifestyle toward the amount money spent mediated by marketing strategy. Int. J. Adv. Sci. Technol. **120**, 97–110 (2018)
14. Chen, Y., Tang, Z.: Speaker recognition of noisy short utterance based on speech frame quality discrimination and three-stage classification model. Int. J. Control Autom. **8**(3), 135–146 (2015)